HHS Public Access

Author manuscript

Psychoneuroendocrinology. Author manuscript; available in PMC 2015 May 11.

Published in final edited form as:

Psychoneuroendocrinology. 2014 April ; 42: 165–177. doi:10.1016/j.psyneuen.2014.01.020.

Glucocorticoid receptor activation impairs hippocampal plasticity by suppressing BDNF expression in obese mice

Marlena Wosiski-Kuhn[1], **Joanna R. Erion**[1], **Elise P. Gomez-Sanchez**[2], **Celso E. Gomez-Sanchez**[2], and **Alexis M. Stranahan**[1,*]

[1]Department of Physiology, Medical College of Georgia, Georgia Regents University, 1120 15th St, Augusta, GA 30912 USA

[2]G.V. (Sonny) Montgomery Veteran's Affairs Medical Center, 1500 Woodrow Wilson Dr, Jackson, MS 39216 USA

Abstract

Diabetes and obesity are associated with perturbation of adrenal steroid hormones and impairment of hippocampal plasticity, but the question of whether these conditions recruit glucocorticoid-mediated molecular cascades that are comparable to other stressors has yet to be fully addressed. We have used a genetic mouse model of obesity and diabetes with chronically elevated glucocorticoids to determine the mechanism for glucocorticoid-induced deficits in hippocampal synaptic function. Pharmacological inhibition of adrenal steroidogenesis attenuates structural and functional impairments by regulating plasticity among dendritic spines in the hippocampus of leptin receptor deficient (db/db) mice. Synaptic deficits evoked by exposure to elevated corticosterone levels in db/db mice are attributable to glucocorticoid receptor-mediated transrepression of AP-1 actions at BDNF promoters I and IV. db/db mice exhibit corticosterone-mediated reductions in brain-derived neurotrophic factor (BDNF), and a change in the ratio of TrkB to P75NTR that silences the functional response to BDNF stimulation. Lentiviral suppression of glucocorticoid receptor expression rescues behavioral and synaptic function in db/db mice, and also reinstates BDNF expression, underscoring the relevance of molecular mechanisms previously demonstrated after psychological stress to the functional alterations observed in obesity and diabetes.

Keywords

corticosterone; hippocampus; long-term potentiation; dentate gyrus; synapse; synaptic plasticity; dendritic spine

Type 2 (insulin resistant) diabetes is a global epidemic, and in the context of an aging population, presents significant challenges related to maintaining both physical independence and cognitive capabilities. Individuals with type 2 diabetes, characterized by elevated fasting glucose and reduced insulin sensitivity, with progression to insulin

*Corresponding author: Alexis M. Stranahan, Medical College of Georgia, Georgia Regents University, Physiology Department, 1120 15th St, room CA3145, Augusta GA 30912, Phone: (706)721-7885, astranahan@gru.edu.

The authors declare no competing financial interests.

insufficiency in the later stages of the disease, develop cognitive impairment earlier and at higher rates relative to individuals with normal glucose and insulin metabolism (Xu et al., 2010). Insulin and glucose are not the only hormonal systems disrupted in diabetes, as dysregulation of adrenal steroid hormone levels and rhythmicity have also been reported in diabetic patients (Bruehl et al., 2007). Data from rodent models also indicate that corticosterone contributes to synaptic and cognitive deficits in type 2 diabetes (Stranahan et al., 2008). However, the extent to which corticosteroids act in the central nervous system or in the periphery to compromise the vulnerable medial temporal lobe circuits underlying memory and cognition in diabetes has yet to be assessed.

Chronic exposure to elevated corticosterone levels suppresses synaptic plasticity in nondiabetic animals, and induces concomitant behavioral deficits, particularly on tests that depend on hippocampal integrity (Kim and Yoon, 1998). However, the vast majority of previous work used systemic administration of corticosterone, which exerts effects on multiple physiological systems, making it difficult to assess the extent to which cognitive impairment following exposure to chronically elevated corticosterone is attributable to a direct role for corticosterone actions on hippocampal neurons, or secondary to effects on another neurologically relevant component of the endocrine milieu. No studies to date have evaluated whether corticosterone acts locally within the hippocampus to impair synaptic and behavioral plasticity in type 2 diabetes, or peripherally to alter another signaling mechanism, leading to cognitive deficits. Given the well-characterized suppression of hippocampal brain-derived neurotrophic factor (BDNF) that occurs following chronic stress-induced elevations in corticosterone levels (Grønli et al., 2006), we hypothesized that prolonged exposure to elevated glucocorticoids might recruit similar pathways in a genetic mouse model of obesity and diabetes. Given that previous studies targeting glucocorticoids in obesity primarily relied on surgical ablation of the adrenal gland (Stranahan et al., 2008; Stranahan et al., 2011), which is not feasible in a clinical setting, the current set of experiments used pharmacological strategies to reduce corticosterone synthesis, in combination with intrahippocampal manipulations of corticosterone levels.

These studies were performed in leptin receptor deficient (db/db) mice, in which diabetes, obesity, and hypercortism arise due to a loss-of-function mutation in the gene encoding the long form of the leptin receptor. Initial experiments using the corticosterone synthesis inhibitor metyrapone revealed that corticosteroid inhibition normalizes hippocampal ultrastructure, synaptic function, and hippocampus-dependent memory. To identify a local role for hippocampal corticosterone as a mediator of neurocognitive impairment, intrahippocampal corticosterone infusions were performed in the presence or absence of systemic metyrapone treatment. These experiments revealed that exposure to elevated corticosterone in the hippocampus impairs synaptic measures and spatial memory. These studies have identified a direct role for corticosterone-mediated reductions in hippocampal neurotrophic support as a mechanism for cognitive impairment in the context of diabetes and obesity.

Methods

Animals and drug treatments

Male C57Bl6/J mice (wildtype) or leptin receptor deficient db/db mice on the same genetic background were obtained from Jackson Laboratories (Bar Harbor, ME, USA) at 5 weeks of age. After acclimating to the vivarium, which is maintained at 28°C and 55% humidity with lights-on at 0600h, mice were treated with metyrapone (100 mg/kg in saline with 20% polyethylene glycol, IP; Tocris Bioscience, Bristol, UK) daily at 1000h to lower and normalize corticosterone levels. All treatments were initiated when the mice were five weeks old. For the initial experiments characterizing the effect of metyrapone on spatial recognition memory, dentate gyrus long-term potentiation (LTP), and dendritic spines visualized by confocal microscopy, groups of (n=6) wildtype mice treated with vehicle, (n=6) wildtype mice treated with metyrapone, (n=6) db/db mice treated with vehicle, and (n=6) db/db mice treated with metyrapone were used. An additional cohort of (n=3) mice per genotype in each drug treatment condition was generated for serial section electron microscopy experiments. For the experiments investigating regulation of BDNF, TrkB, and P75NTR expression, an additional set of (n=8) mice per genotype in each drug treatment condition were used. For studies using intrahippocampal corticosterone treatment together with systemic pharmacological manipulation of glucocorticoids, (n=8) mice from each genotype were randomly assigned to receive intrahippocampal artificial cerebrospinal fluid (ACSF)+systemic vehicle; intrahippocampal corticosterone+systemic vehicle; intrahippocampal ACSF+systemic metyrapone; or intrahippocampal corticosterone +systemic metyrapone. For experiments involving lentiviral manipulation of glucocorticoid receptors, (n=8) wildtype mice treated with the empty vector, (n=10) db/db mice treated with empty vector, and (n=10) db/db mice treated with the glucocorticoid receptor knockdown construct were used. All procedures were approved by the Georgia Regents University Animal Care and Use Committee and followed NIH guidelines.

Stereotaxic surgery

Mice were anesthetized with Isoflurane and implanted with bilateral cannulae (Plastics One) at the following coordinates: anteroposterior, 2.1mm; mediolateral, ±1.5; dorsoventral, 2.1mm (Paxinos and Franklin, 2001). Each side of the bilateral cannula was individually connected to an Alzet minipump for delivery of corticosterone into both hippocampi (Durect Corporation, Cupertino, CA, USA). For intrahippocampal corticosterone experiments, a water-soluble complex of corticosterone and 2-hydroxypropyl-β-cyclodextrin (Sigma-Aldrich, St. Louis, MO, USA) was delivered at 60ng/24hr for two weeks. The vehicle for these experiments consisted of 2-hydroxypropyl-β-cyclodextrin diluted in ACSF at 0.03mg/mL. Cannula placements were verified histologically and through measurement of hippocampal corticosterone levels.

For stereotaxic injection of lentiviral constructs, virus stocks were adjusted to 1×10^6 tu/μl and injected at the following coordinates: AP, −2.1; ML, ± 1.35; and DV, −2.1; and AP, −3.1; ML, ± 2.3; and DV −2.5 (Paxinos and Franklin, 2001). High-titer lentivirus (1 μl) was injected in a constant flow of 0.2μl/min, with the syringe left in place for ten minutes after administration. Injection sites were verified histologically and the efficacy of overexpression

was assessed by measuring glucocorticoid receptor expression in hippocampal homogenates. The GR knockdown vector was purchased from Santa Cruz Biotechnologies (Dallas, TX, USA; sc-35506-V, custom-titered to 1×10^6 transducing units per μl).

Behavioral testing

Mice were tested in a Y-maze apparatus during the dark period between 1800h and 1900h. Testing took place under red light illumination and involved an initial ten minute habituation phase during which the mouse was confined to the start arm of the maze. Following habituation, a guillotine door was lifted and the mouse was permitted to explore until it had fully entered one of the choice arms. Following a complete arm entry, the mouse was again confined to the start arm for a one-minute intertrial interval before the next choice. This sequence was repeated five times, and the number of correct alternations was recorded and expressed relative to the number of trials for statistical analysis.

Enzyme-linked immunosorbent assay and radioimmunoassay

For measurement of hippocampal corticosterone levels, frozen hippocampi were extracted with 50:50 ethyl acetate:hexane. The extracts were evaporated, and the lipid fraction was resuspended in ELISA diluent buffer (Abcam, Cambridge, MA, USA). Serum samples were diluted appropriately for measurement of corticosterone levels by ELISA according to the manufacturer's instructions. Serum aldosterone levels were measured using a radioimmunoassay kit according to the manufacturer's instructions (Siemens Diagnostics, Malvern, PA, USA). Hippocampal BDNF and TrkB protein levels were measured with commercially available kits from Promega (Madison, WI, USA) and Abcam (Cambridge, MA, USA), respectively. Hippocampal P75NTR was measured using a Duoset ELISA development kit from R&D Systems (catalog #DY1157; Minneapolis, MN, USA).

Western blotting and chromatin immunoprecipitation

Protein extraction and quantification of total protein by Bradford assay took place as described (Stranahan et al., 2009). Fifty micrograms of extracted protein were loaded and separated through gel electrophoresis. Proteins were transferred to nitrocellulose membranes, blocked in 5% nonfat milk, and probed with antibodies against BDNF (Abcam, Cambridge, MA, USA), TrkB (Abcam, Cambridge, MA, USA), P75NTR (Cell Signaling Technologies, Danvers, MA, USA), glucocorticoid receptor (Santa Cruz Biotechnologies, Dallas, TX, USA), or mineralocorticoid receptors (generated by Drs. Elise and Celso Gomez-Sanchez). The loading control for whole cell extracts and cytoplasm fractions was β-actin (Sigma-Aldrich, St. Louis, MO, USA), and the loading control for the nuclear extract was TATA-binding protein (Abcam, Cambridge, MA, USA). Primary antibodies were applied at 1:1,000 dilution overnight with shaking at 4C and detected with HRP-conjugated secondaries directed against the appropriate species. Bands were visualized on a chemiluminescence imager and band intensities were quantified using ImageJ. Chromatin immunoprecipitation experiments also followed the manufacturer's instructions (Upstate Biotechnologies, now part of Millipore, Billerica, MA, USA); in brief, rabbit polyclonal antibodies against Fos (Santa Cruz Biotechnologies, Dallas, TX, USA) or normal IgG were used to immunoprecipitate fragmented chromatin from crosslinked extracts. Crosslinking was reversed through proteinase K digestion and the resultant DNA was amplified in the

presence of primers targeting variable BDNF promoter regions. The primer sequences used in the ChIP assays were as follows: promoter I (fwd) TGATCATCACTCACGACCACG, (rev) CAGCCTCTCTGAGCCAGTTACG; promoter IV (fwd), GCGCGGAATTCTGATTCTGGTAAT, (rev), GAGAGGGCTCCACGCTGCCTTGACG.

Electrophysiology

Preparation of hippocampal slices and recording of extracellular field potentials followed previously published methods (Stranahan et al., 2008). In brief, 400 micron slices were cut into a bath of oxygenated artificial cerebrospinal fluid (ACSF) using a Vibratome (Leica, Buffalo Grove, IL, USA). After one hour of recovery, extracellular recordings were made in the ACSF supplemented with 50 micromolar picrotoxin (Sigma-Aldrich, St. Louis, MO, USA). Baseline was set at 50% of the maximal response assessed through input/output curve recordings. Stimuli were delivered at 0.05 Hz during the baseline and posttetanus recordings; tetanic stimulation consisted of a train delivered at 100 Hz for 1 second. BDNF stimulation experiments were carried out according to the methods of Messaoudi and colleagues (1998). In brief, recombinant BDNF (Shenandoah Biotechnologies) was applied to the slices for 15min at 2.0 micrograms per mL, with recording at 0.05Hz throughout, then washed out, with continuous recording over the subsequent 45 minutes. For both types of LTP experiments, the initial 0.5 milliseconds of the dendritic field potential was collected using pClamp version 10.3.4 and analyzed in Clampfit (Molecular Devices, Sunnyvale, CA, USA).

DiI labeling and quantification of dendritic spines

Dendritic spines were visualized using the lipophilic membrane tracer DiI (Molecular Probes, Grand Island, NY, USA) as described (Wosiski-Kuhn and Stranahan, 2012). Five segments per cell were sampled from the secondary and tertiary dendrites of five dentate gyrus granule cells. Cells were visualized using a 63× objective on a Zeiss LSM 510 Meta upright confocal microscope. Cells selected for analysis had somata located in the mid- to superficial portion of the dentate granule cell layer, with dendrites extending into the molecular layer, and every effort was made to select cells with morphological correlates of functional maturity. Spine counts and three-dimensional measurements of the length of the sampled segments were made using Reconstruct software (available at http://synapses.clm.utexas.edu) according to previously published protocols (Wosiski-Kuhn and Stranahan, 2012).

Electron microscopy

For serial section transmission electron microscopy, mice were perfused transcardially under deep Isoflurane anesthesia with fixative containing 2% paraformaldehyde, 2.5% glutaraldehyde, and 2 mM $CaCl_2$ in 0.1M cacodylate buffer, (pH = 7.35). Brain sections were cut at 80 μm thickness on a Vibratome (Leica, Buffalo Grove, IL, USA) and the middle molecular layer was dissected from these sections with the aid of a dissecting microscope. Microdissected regions were embedded according to standard protocols and serial sections were obtained at 60 nm nominal thickness. Serial sections were photographed at 4,000× magnification on a JEOL (Peabody, MA, USA) electron microscope before being aligned for reconstruction using Reconstruct. Five segments were sampled from each series of serial

sections through the dentate middle molecular layer. In order to be selected for reconstruction, dendrites were required to span at least 75 serial sections without exiting the field of view. Dendrites were also matched for their caliber, a measurement derived from the cross-sectional area of the dendrite at the beginning, middle, and end of the segment divided by the number of microtubules within the dendritic shaft at each level. Each spine was manually traced in its entirety; the postsynaptic density was also traced, and postsynaptic density areas were calculated according to the method of Bourne and Harris (Bourne and Harris, 2011). Head diameter measurements were made across the widest extent of the spine head, and spines were subclassified according to their head diameters as being 'mushroom' (head diameter >0.5 μm); 'intermediate' (head diameter <0.05 μm and >0.3 μm); or 'thin' (head diameter <0.3 μm). Spine and synapse numbers were divided by the length of the segment along the Z-axis to generate density measurements. The length of the segment through the Z-axis was corrected for actual section thickness using the cylindrical diameters method as described (Fiala and Harris, 2001).

Histology, stereology, and immunohistochemistry

For analysis of total dentate granule cell numbers, a 1:4 series of 40 micron sections was stained using Cresyl Violet acetate (Sigma-Aldrich, St. Louis, MO, USA) according to previously published methods (Stranahan et al., 2012). Cell counts were made with the aid of StereoInvestigator software, using an XY step size of 150 microns and a dissector height of 10 microns, with 1.5 micron guard zones at the top and bottom of the section; all coefficients of error for this sampling protocol were <0.1. For volumetric analysis of the outer, middle, and inner molecular layers, as well as the granule cell layer and hilus, a 1:4 series of 30 micron sections was processed for Timm staining according to previously published methods (Rapp et al., 1999). Analyses of regional volumes were based on the Cavalieri estimator in StereoInvestigator software (Microbrightfield, Williston, VT, USA).

For immunohistochemical detection of P75NTR, BDNF, TrkB, and GR, mice were perfused transcardially with 4% paraformaldehyde in phosphate buffer. Brains were postfixed for 24hr, cryoprotected in 30% sucrose for an additional 72 hr, and sectioned at 40micron thickness using a freezing microtome (Leica, Buffalo Grove, IL, USA). Sections were maintained in cryoprotectant at −20C prior to immunohistochemical processing. Tissue sections processed for immunohistochemical staining were blocked with 0.3% H_2O_2 in TBS, rinsed, and incubated with primary antibody rabbit anti-P75NTR (Cell Signaling Technologies, Danvers, MA, USA) at 1:1,000 in TBS with 0.25% Tween-20. Sections for TrkB and BDNF labeling were similarly treated prior to incubation with primary antibody rabbit anti-TrkB (1:200; Abcam, Cambridge, MA, USA) or rabbit anti-BDNF (1:500, Abcam, Cambridge, MA, USA) or rabbit anti-GR (1:500, Santa Cruz Biotechnologies, Dallas, TX, USA). Primary antibodies were detected with biotinylated secondaries and visualized with Streptavidin 488 (Molecular Probes, Grand Island, NY, USA). Nuclei were counterstained with DAPI.

Statistics

Behavioral, electrophysiological, ultrastructural, and confocal analysis of DiI-labeled spines from the metyrapone experiments were compared across db/db and wildtype mice treated

with metyrapone or vehicle using 2×2 ANOVA. Protein expression analyses also used 2×2 ANOVA designs with genotype (wildtype or db/db) and drug treatment (metyrapone or vehicle) as fixed factors. In experiments that combined systemic metyrapone treatment with intrahippocampal corticosterone administration, behavioral, electrophysiological, and confocal data were compared using 2×2×2 ANOVAs with genotype (wildtype or db/db), systemic treatment (metyrapone or vehicle) and intrahippocampal treatment (corticosterone or ACSF) as between-subjects factors. For the BDNF-LTP experiments, structural measures were analyzed using 2×2×2 ANOVA with genotype (wildtype or db/db), systemic treatment (metyrapone or vehicle), and BDNF application (BDNF or vehicle) as between-subjects factors. Post hoc planned comparisons were conducted using Bonferroni-corrected t-tests and analyses were carried out using Graphpad Prism v5 or SPSS v18, with statistical significance set at $p<0.05$.

Results

Corticosteroid inhibition reinstates dendritic spine density, LTP, and learning in db/db mice

db/db mice lack the long form of the leptin receptor and are obese and diabetic, with chronically elevated corticosterone levels. Systemic metyrapone administration (100 mg/kg, IP) for fourteen days significantly reduced basal corticosterone levels in db/db mice (for drug × genotype interaction following 2×2 ANOVA, $F_{1,24}=17.48$, $p=0.003$; Figure 1A). db/db mice exhibit impaired learning and memory, particularly on tasks that recruit the hippocampus, (Li et al., 2002; Stranahan et al., 2008) and corticosteroid-dependent impairments in spatial recognition memory were observed in the Y-maze, a hippocampus-dependent task (Conrad et al., 1996). db/db mice treated with vehicle displayed significantly less alternation behavior in the Y-maze, relative to wildtype mice treated with vehicle (for the effect of genotype following 2×2 ANOVA, $F_{1,12}=9.67$, $p=0.009$; Figure 1B). By contrast, db/db mice treated with metyrapone displayed alternation rates that were not significantly different than wildtype mice (for the drug × genotype interaction, $F_{1,12}=4.99$, $p=0.04$; Figure 1B). This pattern is consistent with the hypothesis that lowering corticosterone levels reinstates spatial recognition memory in db/db mice.

Field potential recordings in hippocampal slices further revealed that lowering corticosterone levels pharmacologically rescues long-term potentiation at medial perforant path synapses on dentate gyrus granule cells (for the drug × genotype interaction following 2×2 ANOVA, $F_{1,37}=10.06$, $p=0.003$; Figure 1C). Previous work in this model revealed no changes in the input-output relationship or in the magnitude of presynaptically mediated paired-pulse depression (Stranahan et al., 2008). Taken together with the functional observations in the current experiments, the data support a primarily postsynaptic locus for deficits in plasticity among dentate granule cells in db/db mice. To test the hypothesis that lowering corticosterone levels reinstates postsynaptic structural plasticity in db/db mice, dendritic spines were visualized in slices from metyrapone- and vehicle-treated db/db and wildtype mice using the lipophilic membrane tracer DiI (Figure 1D). db/db mice have fewer dendritic spines than wildtype mice (for the effect of genotype following 2×2 ANOVA, $F_{1,16}=13.03$, $p=0.002$; Figure 1B). Metyrapone treatment normalizes dendritic spine density

along the secondary and tertiary dendritic segments of dentate gyrus granule cells in db/db mice (for the drug × genotype interaction following 2×2 ANOVA, $F_{1,16}$=7.48, p=0.01; Figure 1D).

Dendritic spines are the primary sites for excitatory synapses, and our observation of reduced spine density on DiI-labeled granule neurons is consistent with our functional observations implicating elevated corticosterone levels in the induction of postsynaptic deficits in db/db mice. To further elucidate structural mechanisms for corticosterone-mediated functional deficits, we performed serial section transmission electron microscopy and three-dimensional reconstruction of spines and synapses in the middle molecular layer of the dentate gyrus (Figure 2A). Visual inspection of specific morphological subtypes of spines, classified based on spine head diameter, revealed that thin spines were conspicuously absent on reconstructed dendritic segments from vehicle-treated db/db mice (Figure 2C). Quantification of dendritic spine density and the density of spine subtypes demonstrated that overall spine density and the density of the thin spine subpopulation were reinstated in db/db mice following metyrapone treatment (for the drug × genotype interaction following 2×2 ANOVA on the density of all spines, $F_{1,8}$=10.86, p=0.002; for the drug × genotype interaction following 2×2 ANOVA on the density of thin spines, $F_{1,8}$=4.08, p=0.04; Figure 2B). Vehicle-treated db/db mice had fewer spine synapses than wildtype mice (for the effect of genotype following 2×2 ANOVA, $F_{1,8}$=22.91, p=0.0001) and deficits in synaptic density were also attenuated following metyrapone treatment (for the drug × genotype interaction following 2×2 ANOVA, $F_{1,8}$=8.01, p=0.007; Figure 2D). Changes in synaptic density were selective for spine synapses as no impairment of shaft synapse innervation was observed (Figure 2D).

Vehicle-treated db/db mice had fewer thin spines, and the thin spines that remained had significantly smaller postsynaptic densities (PSDs; Figure 2E), but there was no evidence of synaptic atrophy on thin spines in db/db mice treated with metyrapone (for the drug × genotype interaction following 2×2 ANOVA, $F_{1,8}$=7.26, p=0.009; Figure 2D). There were no differences in the number of spines without PSDs (Figure 2F), or in the number of spines bearing perforated PSDs (Figure 2G). The caliber of the sampled dendrites, defined by the number of microtubules divided by the two dimensional area of the dendritic shaft across multiple serial sections, was comparable between db/db and wildtype mice (Figure 2H), as was the number of mitochondria per sampled dendrite (Figure 2I). Taken together, these observations suggest that thin spines with synapses are especially vulnerable in the context of obesity and diabetes.

Deficits in dendritic spine density are not secondary to global hippocampal atrophy

Because db/db mice are leptin receptor deficient throughout their development, and leptin has been implicated in appropriate morphogenesis of hypothalamic nuclei (Bouret et al., 2004), unbiased stereology and regional morphometry were conducted to determine whether the number or innervation of dentate gyrus granule cells might be altered in db/db mice. There were no gross morphological abnormalities in any hippocampal subfield on Cresyl-violet stained sections from db/db mice. Unbiased stereology revealed comparable total cell numbers in the dentate gyrus granule cell layer (t-test comparing wildtype and db/db mice,

t_{14}=0.46, p=0.64; Figure S1A). Quantitative morphometry of Timm-stained sections delineating the outer, middle, and inner components of the dentate molecular layer also suggests that the anatomical innervation of dentate granule cells is comparable between db/db and wildtype mice (Figure S1B; for the outer molecular layer, t_{14}=0.21, p=0.83; for the middle, t_{14}=0.35, p=0.74; for the inner, t_{14}=.21, p=0.78; all statistics derived from t-tests). Moreover, the volume of the dentate granule cell layer and hilus were similar between db/db and wildtype mice (Figure S1B; for the granule cell layer, t_{14}=1.08, p=0.29; for the hilus, t_{14}=0.66, p=0.52; statistics derived from t-tests). These structural observations are consistent with the absence of alterations in total dendritic length or complexity previously reported among hippocampal dentate granule neurons in db/db mice (Stranahan et al., 2009). The outcome of these morphological studies at the level of light microscopy suggests that hippocampal neuroanatomy is relatively normal in the absence of leptin receptor signaling.

Glucocorticoid receptor binding to the AP-1 transcription factor complex reduces BDNF expression in db/db mice

Although there is significant consensus surrounding the negative regulation of BDNF by prolonged activation of glucocorticoid receptors, conflicting reports exist in the literature surrounding alterations in hippocampal gluco- and mineralocorticoid receptor expression in leptin deficient rodent models (Jöhren et al., 2007; Campbell et al., 2010). To determine whether the expression or localization of gluco- and mineralocorticoid receptors might differ in db/db mice, cellular fractionation experiments were carried out to analyze the expression and localization of receptors for corticosterone. Consistent with their tonic occupation by corticosterone due to high affinity binding, significant nuclear localization of MR was detected in both wildtype and db/db mice, whether they were treated with metyrapone or vehicle (Figure 3A). However, the nuclear localization of the lower-affinity glucocorticoid receptor, which is activated following stress and at certain points during the circadian cycle, was significantly greater in vehicle-treated db/db mice, relative to metyrapone-treated db/db mice or wildtype mice ($F_{1,10}$=9.67, p=0.001; Figure 3A). Cytosolic levels of MR and GR revealed the inverse pattern, suggesting that vehicle-treated db/db mice exhibit increases in nuclear GR, with possible consequences for gene transcription.

Chronic exposure to stress-induced elevations in corticosterone levels reduces hippocampal BDNF expression via transrepression. Nuclear glucocorticoid receptor dimers adhere to the AP-1 transcription factor complex, and thereby reduce expression of AP-1 target genes, such as BDNF. To evaluate the extent to which nuclear GR might be interfering with AP-1 actions at different BDNF promoters, coimmunoprecipitation analysis was performed using antibodies against GR and Fos, a component of the AP-1 heteromer. This assay revealed that nuclear GR associates with Fos in vehicle-treated db/db mice, but not in metyrapone-treated db/db mice or wildtype mice (Figure 3B; $F_{1,12}$=5.61, p=0.04). This observation suggests that corticosterone-mediated increases in nuclear GR in db/db mice are accompanied by association with, and possibly sequestration of, the AP-1 transcription factor complex (Figure 3B). To examine the possible relevance of reductions in AP-1 mediated transcriptional activity for BDNF expression, chromatin immunoprecipitation and quantitative RT-PCR was carried out in hippocampal tissue from db/db and wildtype mice treated with metyrapone or vehicle. Fos protein was reliably bound to BDNF promoters I

and IV, both of which contain AP-1 binding sites, in hippocampal tissue from wildtype mice. By contrast, this same protocol detected substantially less expression of BDNF promoters I and IV in Fos precipitates from vehicle-treated db/db mice (Figure 3B; for promoter I, $F_{1,12}$=14.16, p=0.002; for promoter IV, $F_{1,12}$=8.95, p=0.01). Systemic inhibition of corticosterone synthesis reinstituted the association between Fos and BDNF promoters I and IV in db/db mice, in support of a functional role for glucocorticoid receptors as transrepressors of AP-1 activity at promoter regions mediating activity-dependent expression of BDNF.

Metyrapone rescues brain-derived neurotrophic factor expression in db/db mice

Brain-derived neurotrophic factor (BDNF) is an obligatory contributor to structural and functional plasticity. Inhibition of corticosterone synthesis with metyrapone reinstated BDNF protein levels in the hippocampus of db/db mice (for the drug × genotype interaction following 2×2 ANOVA, $F_{1,30}$=7.31, p=0.01; Figure 3C). Loss of dentate gyrus BDNF protein expression in vehicle-treated db/db mice and reinstatement with metyrapone treatment was also evident in sections processed for immunohistochemical detection of BDNF (Figure 3C). db/db mice also exhibit reinstatement of TrkB protein expression following metyrapone treatment (for the drug × genotype interaction following 2×2 ANOVA, $F_{1,31}$=6.92, p=0.01; Figure 3D). Deficits in dentate gyrus TrkB immunoreactivity were evident on histological sections from vehicle-treated db/db mice, but metyrapone-treated db/db mice were identical to wildtype (Figure 3D). BDNF binds to both its high-affinity receptor, TrkB, and to the P75 neurotrophin receptor (P75NTR), with lower affinity. BDNF-P75NTR signaling constrains plasticity (Zagrebelsky et al., 2005), so we next evaluated expression of P75NTR, to determine whether alterations in the balance between BDNF-TrkB and BDNF-P75NTR might be occurring in the db/db mouse hippocampus. db/db mice had elevated levels of hippocampal P75NTR, detectable using enzyme-linked immunosorbent assay (Figure 3E; for the drug × genotype interaction following 2×2 ANOVA, $F_{1,32}$=16.83, p=0.003). Metyrapone attenuated the increase in P75NTR in db/db mice, suggesting that elevated corticosterone levels act by shunting BDNF away from TrkB and towards P75NTR, with deleterious consequences for synaptic structure and function.

Synaptic potentiation was assessed following BDNF application (BDNF-LTP) in parallel with visualization of dendritic spines (Messaoudi et al., 1998). Vehicle-treated db/db mice did not exhibit BDNF-LTP, but metyrapone-treated db/db mice showed robust synaptic responses to exogenous BDNF (Figure 3F; for the drug × genotype interaction following 2×2 ANOVA, $F_{1,35}$=4.22, p=0.04). Hippocampal slices from db/db and wildtype mice that had been treated with metyrapone or vehicle were exposed to exogenous BDNF (2 μg/ml), followed by assessment of dendritic spine density along the secondary and tertiary dendrites of dentate gyrus granule cells, to determine whether lowering corticosterone might reinstate BDNF-induced structural plasticity. Exposure to exogenous BDNF enhanced dendritic spine density in wildtype mice, irrespective of whether they were treated with metyrapone or vehicle (for the effect of BDNF on spine density following 2×2×2 ANOVA, $F_{1,18}$=8.04, p=0.01; Figure 3G). db/db mice treated with vehicle had fewer spines at baseline, and failed to respond to BDNF with enhanced spine density, but metyrapone treatment reinstated BDNF-evoked increases in spine density in db/db mice (for the drug × genotype×BDNF

interaction following 2×2×2 ANOVA, $F_{1,18}$=6.76, p=0.02; Figure 3G), in support of the assertion that exposure to elevated corticosterone levels suppresses hippocampal function in db/db mice by weakening neurotrophic support of synaptic plasticity.

Hippocampal exposure to elevated corticosterone levels evokes synaptic and cognitive deficits

Metyrapone reduces corticosterone synthesis by inhibiting the enzyme 11β-hydroxylase, which is required for conversion of 11-deoxycorticosterone to corticosterone. However, metyrapone also suppresses the activity of enzymes required for aldosterone synthesis, and in the current experiment, metyrapone treatment attenuated elevations in serum aldosterone observed in vehicle-treated db/db mice (pg/mL, mean±s.e.m; wt/Veh=85.24±8.77, db/Veh=493.53±70.02, wt/Met=39.68±7.59, db/Met=236.64±26.78; for the drug × genotype interaction following 2×2 ANOVA, $F_{1,26}$=6.77, p=0.02). This opens the possibility that cognitive and synaptic reinstatement following metyrapone treatment might be attributable to changes in aldosterone, rather than alterations in corticosterone.

To address whether hippocampal exposure to elevated corticosterone levels was sufficient to evoke cognitive and synaptic impairments, central and peripheral corticosterone levels were independently manipulated through the combination of systemic metyrapone and intrahippocampal corticosterone infusions (Figure 4A). These experiments were performed in both wildtype and db/db mice, to determine the consequences of direct exposure to elevated glucorticoid levels for hippocampal neuroplasticity. Metyrapone treatment lowered circulating corticosterone levels comparably in db/db mice receiving intrahippocampal infusions of ACSF or corticosterone (for the effect of drug following 2×2×2 ANOVA, $F_{1,29}$=40.23, p=0.001; Figure 4B). Corticosterone was delivered intrahippocampally at 60ng/24hr; this dose was selected in order to recapitulate hippocampal corticosterone levels detected in pilot experiments measuring hippocampal corticosterone levels in intact wildtype and db/db mice. Quantification of hippocampal corticosterone levels in the cannulated mice revealed that mice infused intrahippocampally with corticosterone have elevated levels of hippocampal corticosterone (for the effect of intrahippocampal corticosterone following 2×2×2 ANOVA, $F_{1,21}$=5.90, p=0.02; Figure 4B). These assays demonstrate successful independent manipulation of central and systemic corticosterone levels in both db/db and wildtype mice (Figure 4B).

Behaviorally, intrahippocampal corticosterone treatment impaired spatial recognition memory performance in metyrapone-treated db/db mice (Figure 4C; for the interaction between systemic drug treatment and intrahippocampal drug treatment in db/db mice following 2×2 ANOVA, $F_{1,32}$=8.00, p=0.008), and in wildtype mice (for the effect of intrahippocampal corticosterone in wildtype mice following 2×2 ANOVA, $F_{1,32}$=6.13, p=0.01), suggesting that hippocampal exposure to elevated glucocorticoids is sufficient to evoke cognitive deficits. Visualization of DiI-labeled dendritic spines on dentate gyrus granule neurons and quantification of dendritic spine density provided additional support for intrahippocampally elevated corticosterone levels as a mediator for synaptic deficits. Metyrapone-treated db/db mice infused with ACSF exhibit normalization of dendritic spine density, while intrahippocampal corticosterone treatment recapitulates deficits in

metyrapone-treated db/db mice. (Figure 4D–E; for the interaction between systemic drug treatment and intrahippocampal drug treatment in db/db mice following 2×2 ANOVA, $F_{1,12}$=6.25, p=0.03). Intrahippocampal corticosterone infusions also impaired dendritic spine density in wildtype mice irrespective of systemic glucocorticoid manipulation (for the effect of intrahippocampal corticosterone in wildtype mice following 2×2 ANOVA, $F_{1,24}$=18.89, p=0.001; Figure 4D–E).

Extracellular recordings in hippocampal slices revealed that intrahippocampal exposure to elevated corticosterone reduces LTP in metyrapone-treated db/db mice and in wildtype mice (Figure 4F–G; for the interaction between systemic drug treatment and intrahippocampal drug treatment in db/db mice following 2×2 ANOVA, $F_{1,38}$=5.55, p=0.02; for the effect of intrahippocampal corticosterone in wildtype mice following 2×2 ANOVA, $F_{1,50}$=8.72, p=0.005), indicating that intrahippocampal corticosterone evokes synaptic functional impairment across genotypes. Quantification of hippocampal BDNF protein expression following intrahippocampal corticosterone treatment revealed that, consistent with our structural and functional outcomes, reinstatement of high hippocampal corticosterone levels reduces BDNF in metyrapone-treated db/db mice (Figure 4H; for the interaction between systemic drug treatment and intrahippocampal drug treatment in db/db mice following 2×2 ANOVA, $F_{1,38}$=6.54, p=0.001; for the effect of intrahippocampal corticosterone in wildtype mice following 2×2 ANOVA, $F_{1,50}$=8.944, p=0.005). Taken together, these observations in db/db and wildtype mice suggest that hippocampal exposure to elevated glucocorticoids is sufficient to evoke cognitive and synaptic deficits, and implicate changes in hippocampal BDNF expression as a downstream mechanism.

Glucocorticoid receptor hyperactivity contributes to neurocognitive impairment in db/db mice

Because GR-mediated transrepression of BDNF was implicated as a mechanism for synaptic dysfunction in db/db mice, lentiviral particles bearing GR shRNA were next used to knock down hippocampal GR expression. Analysis of whole hippocampal homogenates revealed successful reductions in GR protein, with no effect on MR expression (Figure 5A–B). Immunofluorescent detection of the GFP reporter (Figure 5A) and immunolabeling for GR (Figure 5B) revealed that the knockdown was specific to the dentate gyrus. Detection of dendritic spines on dentate gyrus granule cells revealed that activation of hippocampal GR mediates structural deficits in the db/db mouse model of genetic obesity ($F_{2,35}$=25.29, p=0.001; Figure 5C). Likewise, assessment of tetanic stimulation-induced LTP ($F_{2,40}$=6.15, p=0.005; Figure 5D) indicated that functional plasticity was normalized following reductions in GR. Behavioral analysis of spatial recognition memory in the Y-maze revealed that GR knockdown improved hippocampus-dependent memory in db/db mice ($F_{2,26}$=22.49, p=0.001; Figure 5E). Fractionation experiments demonstrated that nuclear GR is reduced by the knockdown vector, and co-immunoprecipitation experiments revealed that lentiviral knockdown of GR reduced its association with Fos, a component of the AP-1 transcription factor complex. Immunoprecipitation of Fos and analysis of BDNF promoters I and IV by QPCR demonstrated that knocking down GR re-established the physical association between Fos protein and BDNF promoters in db/db mice (Figure 5G; for PI, $F_{2,17}$=12.43, p=0.001; for PIV, $F_{2,17}$=4.32, p=0.007). Moreover, GR knockdown reinstated hippocampal

BDNF protein expression ($F_{2,23}$=6.92, p=0.004; Figure 5H), suggesting that activation of hippocampal GR suppresses synaptic and behavioral function in db/db mice by reducing BDNF.

Discussion

These studies have identified a direct role for corticosterone-mediated reductions in hippocampal BDNF as a mechanism for synaptic and cognitive impairment in a genetic mouse model of obesity and type 2 diabetes. Pharmacological suppression of corticosterone synthesis improves metabolism and memory, and effects on learning and synaptic plasticity are attributable to the local actions of corticosterone in the hippocampus. Hippocampal exposure to elevated corticosterone levels reduces BDNF expression, and biases BDNF signaling away from the pro-plasticity TrkB receptor in favor of the pro-death receptor P75NTR. These effects appear to be mediated by glucocorticoid receptor activation, leading to subsequent reductions in hippocampal BDNF expression, with associated deficits in cognition and synaptic plasticity.

Loss of spines was particularly prominent among thin dendritic spines, which are distinct from filopodia in that they possess a synapse. Spine loss also occurred in the population of intermediate spines, which comprise both stubby spines defined as having a 1:1 ratio of length to head diameter (Bourne and Harris, 2008), and spines that lack such a ratio but do not meet morphological criteria for either thin or mushroom spines. While the functional significance of each morphological class of dendritic spines remains mysterious, there is evidence to suggest that turnover among thin spines is important for plasticity (Holtmaat et al., 2005). Moreover, previous work from our lab has shown that spine turnover is involved in early LTP in the hippocampal dentate gyrus (Wosiski-Kuhn and Stranahan, 2012). Rather than representing a unique population, thin spines likely represent one point along a continuum of spine morphologies, and future studies using time-lapse imaging will be required to determine whether elevated glucocorticoids mediate dynamic fluctuations in spine morphology in obesity and diabetes. Because no commensurate increases in mushroom spine density were observed, glucocorticoid-mediated spine loss in db/db mice is not likely to occur as a result of accelerated transitions from thin to mushroom. Thin and intermediate spines are more likely to disappear as a result of diabetes-induced corticosterone exposure due to the loss of neurotrophic support required to promote their stabilization and expansion. Given previous work surrounding the importance of promoter I- and IV-mediated transcriptional activation of BDNF for activity-dependent plasticity (Pruunsild et al., 2011), this seems the most likely explanation, although additional studies manipulating BDNF expression in db/db mice will be needed to fully characterize the functional relevance of this pathway.

The synaptic and behavioral consequences of metyrapone treatment could be attributable to changes in adrenal production of corticosterone, or alterations in expression or activity of 11beta hydroxysteroid dehydrogenase 1 (11betaHSD1) in the hippocampus. 11betaHSD1 reactivates corticosterone from inactive cortisone, and its actions are also suppressed following metyrapone treatment (Sampath-Kumar et al., 1997). Given the recognized role of 11betaHSD1 as a local amplifier of hippocampal corticosterone levels (Yau and Seckl,

2012), and previous studies demonstrating that 11betaHSD1 inhibition improves cognition in humans with type 2 diabetes (Sandeep et al., 2004), a potential role for 11betaHSD1 in the synaptic alterations observed in the current report is not only possible, but likely. The question of whether metyrapone acts by attenuating adrenal corticosterone synthesis, or by blunting the activity of 11betaHSD1 in the hippocampus, remains to be addressed, but changes at either of these levels will generate the same outcome. Specifically, reductions in hypercortism at the adrenal level or 11betaHSD1 in the hippocampus lead to reductions in glucocorticoid receptor activation, reinstatement of BDNF signaling, and normalization of synaptic and cognitive function.

Given the observation that metyrapone attenuates not only corticosterone synthesis, but also aldosterone levels in db/db mice, there remains the possibility that changes in aldosterone could be contributing to the behavioral and synaptic outcomes. However, this is unlikely given that prior work in insulin-deficient diabetes suggests that aldosterone application in hippocampal slices prevents, rather than promotes, plasticity deficits (Stranahan et al., 2010). Because metyrapone treatment lowers aldosterone levels in addition to lowering corticosterone levels, and previous work suggests that aldosterone enhances hippocampal excitability (Karst et al., 2005), the changes observed in serum samples in the current experiment do not support a role for reductions in circulating aldosterone as a mechanism for reinstatement of cognitive and synaptic function following metyrapone treatment.

The suppression of neuroplasticity and learning observed following chronic infusions of corticosterone contrasts with the enhancement of learning (Roozendaal et al., 2006) and BDNF/TrkB signaling (Jeanneteau et al., 2008) reported following acute exposure to elevated glucocorticoids. Both enhanced neuroplasticity following acute elevations in glucocorticoids and impaired neuroplasticity following chronic exposure to elevated glucocorticoids likely arise from a direct interaction between glucocorticoid receptors and the BDNF receptor, TrkB (Jeanneteau et al., 2008; Numakawa et al., 2009). However, possible interactions between TrkB and gluco- or mineralocorticoid receptors have not yet been explored in the context of type 2 diabetes. Because diabetes, cognitive impairment, and stress-related neuropsychiatric disorders show significant overlap in the epidemiological literature (Golden et al., 2008), it is possible that treatment strategies designed to attenuate the actions of glucocorticoids in the brain and/or promote BDNF signaling via the TrkB receptor might represent a potential avenue for treatment of this pathological triumvirate.

Supplementary Material

Refer to Web version on PubMed Central for supplementary material.

Acknowledgements

We are grateful to Robert Smith and Libby Perry from the Georgia Regents University Electron Microscopy Core Facility for their assistance with the serial section transmission electron microscopy experiments. This project was supported by start-up funds from the Medical College of Georgia.

References

Bouret SG, Draper SJ, Simerly RB. Trophic action of leptin on hypothalamic neurons that regulate feeding. Science. 2004; 304:108–110. [PubMed: 15064420]

Bourne JN, Harris KM. Coordination of size and number of excitatory and inhibitory synapses results in a balanced structural plasticity along mature hippocampal CA1 dendrites during LTP. Hippocampus. 2011; 21:354–373. [PubMed: 20101601]

Bourne JN, Harris KM. Balancing structure and function at hippocampal dendritic spines. Annu Rev Neurosci. 2008; 31:47–67. [PubMed: 18284372]

Bruehl H, Rueger M, Dziobek I, Sweat V, Tirsi A, Javier E, Arentoft A, Wolf OT, Convit A. Hypothalamic-pituitary-adrenal axis dysregulation and memory impairments in type 2 diabetes. J Clin Endocrinol Metab. 2007; 92:2439–2445. [PubMed: 17426095]

Campbell JE, Király MA, Atkinson DJ, D'souza AM, Vranic M, Riddell MC. Regular exercise prevents the development of hyperglucocorticoidemia via adaptations in the brain and adrenal glands in male Zucker diabetic fatty rats. Am J Physiol Regul Integr Comp Physiol. 2010; 299:R168–R176. [PubMed: 20393161]

Conrad CD, Galea LA, Kuroda Y, McEwen BS. Chronic stress impairs rat spatial memory on the Y maze, and this effect is blocked by tianeptine pretreatment. Behav Neurosci. 1996; 110:1321–1334. [PubMed: 8986335]

Fiala JC, Harris KM. Cylindrical diameters method for calibrating section thickness in serial electron microscopy. J Microsc. 2001; 202:468–472. [PubMed: 11422668]

Golden SH, Lazo M, Carnethon M, Bertoni AG, Schreiner PJ, Diez Roux AV, Lee HB, Lyketsos C. Examining a bidirectional association between depressive symptoms and diabetes. JAMA. 2008; 299:2751–2759. [PubMed: 18560002]

Grønli J, Bramham C, Murison R, Kanhema T, Fiske E, Bjorvatn B, Ursin R, Portas CM. Chronic mild stress inhibits BDNF protein expression and CREB activation in the dentate gyrus but not in the hippocampus proper. Pharmacol Biochem Behav. 2006; 85:842–849. [PubMed: 17204313]

Holtmaat AJ, Trachtenberg JT, Wilbrecht L, Shepherd GM, Zhang X, Knott GW, Svoboda K. Transient and persistent dendritic spines in the neocortex in vivo. Neuron. 2005; 45:279–291. [PubMed: 15664179]

Jeanneteau F, Garabedian MJ, Chao MV. Activation of Trk neurotrophin receptors by glucocorticoids provides a neuroprotective effect. Proc Natl Acad Sci U S A. 2008; 105:4862–4867. [PubMed: 18347336]

Jöhren O, Dendorfer A, Dominiak P, Raasch W. Gene expression of mineralocorticoid and glucocorticoid receptors in the limbic system is related to type-2 like diabetes in leptin-resistant rats. Brain Res. 2007; 1184:160–167. [PubMed: 17945204]

Karst H, Berger S, Turiault M, Tronche F, Schütz G, Joëls M. Mineralocorticoid receptors are indispensable for nongenomic modulation of hippocampal glutamate transmission by corticosterone. Proc Natl Acad Sci U S A. 2005; 102:19204–19207. [PubMed: 16361444]

Kim JJ, Yoon KS. Stress: metaplastic effects in the hippocampus. Trends Neurosci. 1998; 21:505–509. [PubMed: 9881846]

Li XL, Aou S, Oomura Y, Hori N, Fukunaga K, Hori T. Impairment of long-term potentiation and spatial memory in leptin receptor-deficient rodents. Neuroscience. 2002; 113:607–615. [PubMed: 12150780]

Messaoudi E, Bârdsen K, Srebro B, Bramham CR. Acute intrahippocampal infusion of BDNF induces lasting potentiation of synaptic transmission in the rat dentate gyrus. J Neurophysiol. 1998; 79:496–499. [PubMed: 9425220]

Numakawa T, Kumamaru E, Adachi N, Yagasaki Y, Izumi A, Kunugi H. Glucocorticoid receptor interaction with TrkB promotes BDNF-triggered PLC-gamma signaling for glutamate release via a glutamate transporter. Proc Natl Acad Sci U S A. 2009; 106:647–652. [PubMed: 19126684]

Paxinos, G.; Franklin, KBJ. The mouse brain in stereotaxic coordinates. second Ed.. San Diego: Academic Press; 2001.

Pruunsild P, Sepp M, Orav E, Koppel I, Timmusk T. Identification of cis-elements and transcription factors regulating neuronal activity-dependent transcription of human BDNF gene. J Neurosci. 2011; 31:3295–3308. [PubMed: 21368041]

Rapp PR, Stack EC, Gallagher M. Morphometric studies of the aged hippocampus: I. Volumetric analysis in behaviorally characterized rats. J Comp Neurol. 1999; 403:459–470. [PubMed: 9888312]

Roozendaal B, Okuda S, Van der Zee EA, McGaugh JL. Glucocorticoid enhancement of memory requires arousal-induced noradrenergic activation in the basolateral amygdala. Proc Natl Acad Sci U S A. 2006; 103:6741–6746. [PubMed: 16611726]

Sampath-Kumar R, Yu M, Khalil MW, Yang K. Metyrapone is a competitive inhibitor of 11beta-hydroxysteroid dehydrogenase type 1 reductase. J Steroid Biochem Mol Biol. 1997; 62:195–199. [PubMed: 9393954]

Sandeep TC, Yau JL, MacLullich AM, Noble J, Deary IJ, Walker BR, Seckl JR. 11Beta-hydroxysteroid dehydrogenase inhibition improves cognitive function in healthy elderly men and type 2 diabetics. Proc Natl Acad Sci U S A. 2004; 101:6734–6739. [PubMed: 15071189]

Stranahan AM, Arumugam TV, Lee K, Cutler RG, Egan JP, Mattson MP. Diabetes impairs hippocampal function through glucocorticoid-mediated effects on new and mature neurons. Nature Neuroscience. 2008; 11:309–317.

Stranahan AM, Arumugam TV, Lee K, Mattson MP. Mineralocorticoid receptor activation restores medial perforant path LTP in diabetic rats. Synapse. 2010; 64:528–532. [PubMed: 20196138]

Stranahan AM, Jiam NT, Spiegel AM, Gallagher M. Aging reduces total neuron number in the dorsal component of the rodent prefrontal cortex. J Comp Neurol. 2012; 520:1318–1326. [PubMed: 22020730]

Stranahan AM, Lee K, Martin B, Maudsley S, Golden E, Cutler RG, Mattson MP. Voluntary exercise and caloric restriction enhance hippocampal dendritic spine density and BDNF levels in diabetic mice. Hippocampus. 2009; 19:951–961. [PubMed: 19280661]

Wosiski-Kuhn M, Stranahan AM. Transient increases in dendritic spine density contribute to dentate gyrus long-term potentiation. Synapse. 2012; 66:661–664. [PubMed: 22314918]

Xu W, Caracciolo B, Wang HX, Winblad B, Bäckman L, Qiu C, Fratiglioni L. Accelerated progression from mild cognitive impairment to dementia in people with diabetes. Diabetes. 2010; 59:2928–2935. [PubMed: 20713684]

Yau JL, Seckl JR. Local amplification of glucocorticoids in the aging brain and impaired spatial memory. Front Aging Neurosci. 2012; 4:24. [PubMed: 22952463]

Zagrebelsky M, Holz A, Dechant G, Barde YA, Bonhoeffer T, Korte M. The p75 neurotrophin receptor negatively modulates dendrite complexity and spine density in hippocampal neurons. J Neurosci. 2005; 25:9989–9999. [PubMed: 16251447]

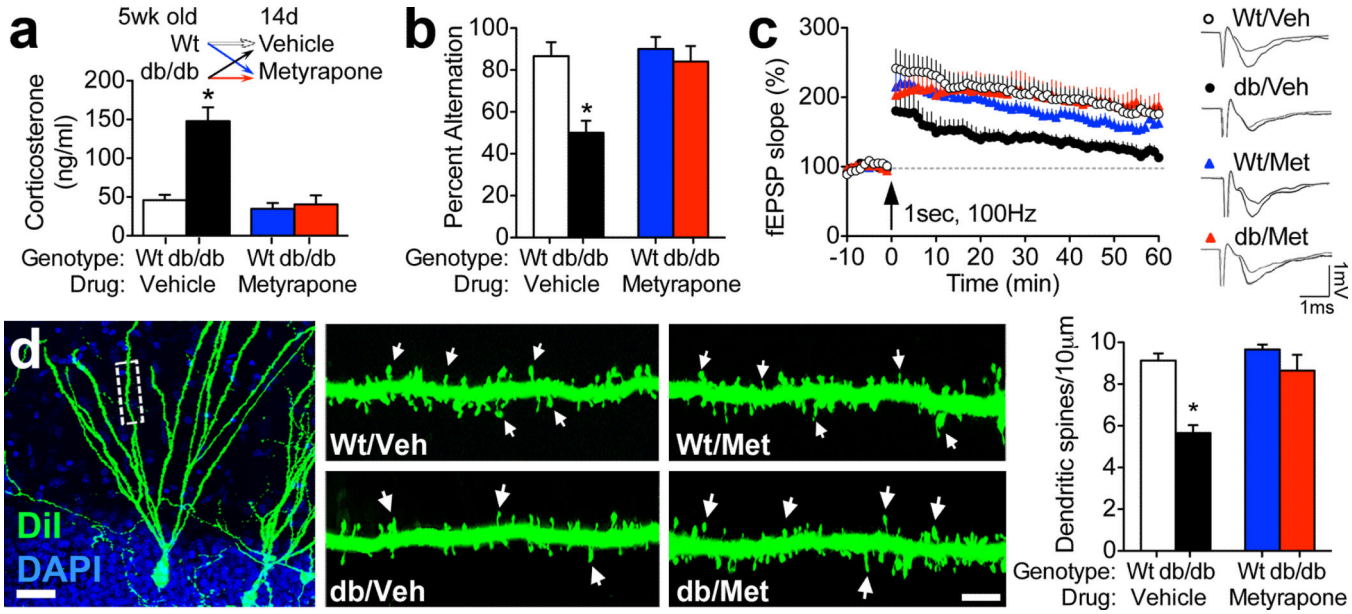

Figure 1. Pharmacological inhibition of corticosterone synthesis reinstates synaptic structural and functional plasticity and rescues spatial learning in db/db mice

(A), Top panel shows the experimental design; male wildtype and leptin receptor deficient db/db mice were administered the corticosterone synthesis inhibitor metyrapone (Met; 100 mg/kg, IP) or vehicle daily for fourteen days. Bottom panel shows serum corticosterone values following this treatment. (B), db/db mice exhibit spatial recognition memory impairments that are prevented by metyrapone treatment. (C), Dentate gyrus long-term potentiation is impaired in db/Veh mice and intact in db/Met mice. (D), Left panel depicts a dentate gyrus granule neuron visualized using DiI labeling (Scale bar=20µm). Middle and right panels show dendritic segments from db/db and wildtype mice treated with metyrapone or vehicle, with dendritic spines indicated by arrows. Scalebar=5µm. Graph (far right) shows the results of spine density measurements indicating that metyrapone-treated db/db mice have significantly more spines than vehicle-treated db/db mice. For all graphs, asterisk (*) indicates statistical significance at $p<0.05$ relative to vehicle-treated wildtype mice following 2×2 ANOVA with Bonferroni's post hoc. Error bars represent the s.e.m. For color interpretation, the reader is referred to the web version of this article.

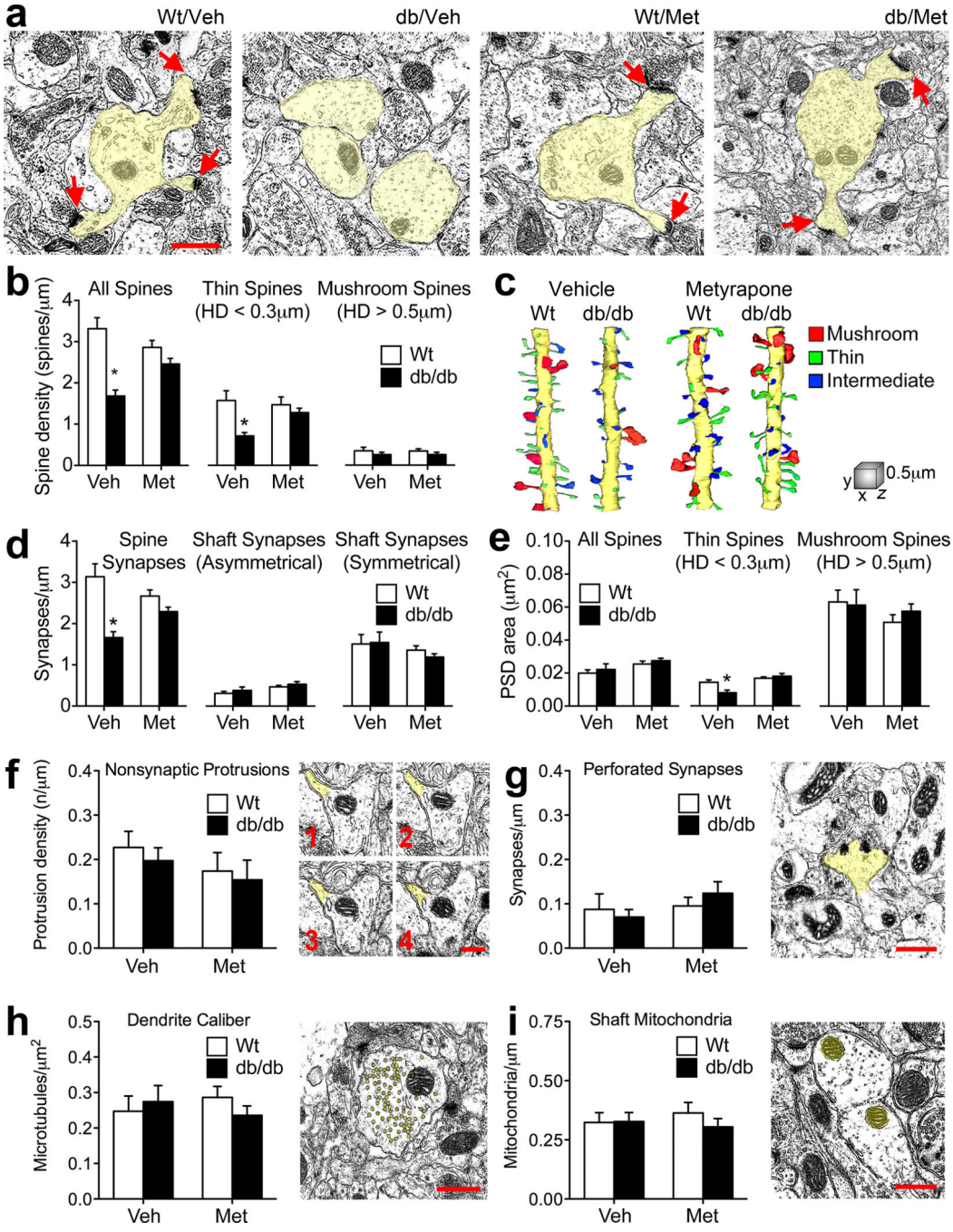

Figure 2. Ultrastructural evidence for corticosterone-mediated reductions in thin spines as a structural correlate of functional impairment in db/db mice

(A), Electron micrographs (with dendrites highlighted in yellow) from the middle of the dentate molecular layer in a vehicle-treated wildtype mouse (Wt/Veh); a vehicle-treated db/db mouse (db/Veh); a metyrapone-treated wildtype mouse (Wt/Met), and a metyrapone-treated db/db mouse (db/Met). Scale bar=0.5μm, arrows indicate dendritic spines. (B), Pharmacological inhibition of adrenal steroidogenesis attenuates spine density deficits in db/db mice, particularly among thin spines. (C), Reconstruction of dendritic segments from serial sections revealed that db/Veh mice have deficits in thin spine density that are

attenuated with metyrapone treatment. Scale cube, XYZ=1μm. (D), Metyrapone treatment normalizes spine synapse density, without influencing shaft synapses in db/db mice. (E), Thin spines exhibit corticosterone-mediated synaptic atrophy in db/db mice. (F), There were no differences in the density of filopodia, defined as thin spines lacking a synapse, across genotypes and treatment conditions. (G), No effect of drug or genotype on the density of spines bearing perforated synapses. (H), Dendrite caliber, defined as the 2-dimensional area of the dendritic shaft at the start, middle, and end of the segment divided by the number of microtubules within the shaft at that position on the Z-axis, was also similar between db/db and wildtype mice. (I), There was no change in the density of mitochondria in the dendritic shaft. For all graphs, asterisks (*) indicate statistical significance at $p<0.05$ relative to vehicle-treated wildtype mice following 2×2 ANOVA with Bonferroni's post hoc. Error bars represent the s.e.m. For color interpretation, the reader is referred to the web version of this article.

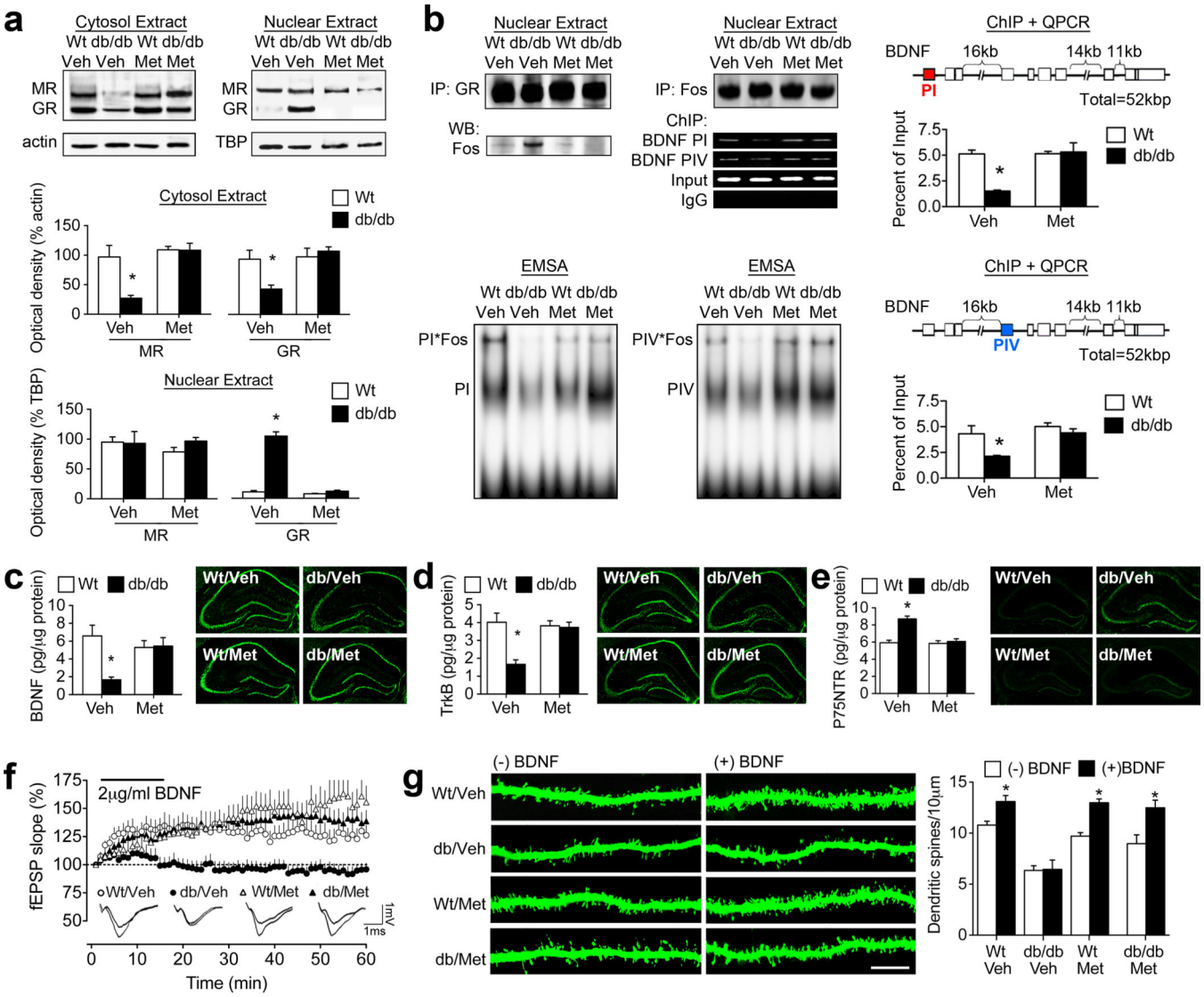

Figure 3. Lowering corticosterone levels normalizes BDNF expression and reinstates functional responses to exogenous BDNF

(A), Vehicle-treated db/db mice exhibit increases in nuclear GR, with commensurate reductions in cytosolic GR, consistent with hippocampal exposure to high levels of corticosterone. Systemic inhibition of corticosterone synthesis reverses this pattern. (B), Exposure to elevated corticosterone levels reduces hippocampal BDNF due to glucocorticoid receptor-mediated transrepression of AP-1 at BDNF promoters I and IV. Nuclear GR co-immunoprecipitate with Fos, a component of the AP-1 transcription factor complex, in vehicle-treated db/db mice, but not in wildtype mice or db/db mice treated with metyrapone. Further analysis by chromatin immunoprecipitation and RTPCR reveals that BDNF promoter I and IV sequences are more abundant in Fos precipitates from wildtype mice, relative to vehicle-treated db/db mice. The association between Fos, a component of the AP-1 transcription factor complex, and BDNF promoters I and IV was reinstated by metyrapone treatment, as assessed by ChIP and EMSA. (C), db/db mice treated with vehicle have reduced hippocampal BDNF expression, but metyrapone-treated db/db mice exhibit

levels of endogenous BDNF that are comparable to wildtype mice. Micrographs show immunostaining for BDNF. (D), db/db mice exhibit reduced expression of the high-affinity BDNF receptor, TrkB, and treatment with metyrapone reverses this deficiency. Micrographs show immunostaining for TrkB. (E), BDNF also binds to P75NTR, thereby constraining plasticity (Zagrebelsky et al., 2005); db/db mice have more hippocampal P75NTR in the vehicle-treated condition, and this is reversed by metyrapone treatment. Micrographs show immunostaining for P75NTR. (F), Vehicle-treated db/db mice fail to exhibit BDNF-LTP, while metyrapone-treated db/db mice exhibit robust BDNF-LTP. Analysis of field excitatory postsynaptic potential (fEPSP) slopes during the last ten minutes of the recording reveals that BDNF-LTP is impaired in vehicle-treated db/db mice and intact in metyrapone-treated db/db mice. (G), Analysis of dendritic spine densities in the presence or absence of BDNF stimulation revealed that BDNF-induced enhancement of dendritic spine density is blocked by elevated corticosterone levels in db/db mice. For graphs in (A-E), asterisk (*) indicates significance at $p<0.05$ relative to vehicle-treated wildtype mice following 2×2 ANOVA. In panel (G), asterisk indicates significant effect of BDNF stimulation following 2×2×2 ANOVA with Bonferonni's post hoc. For color interpretation, the reader is referred to the web version of this article.

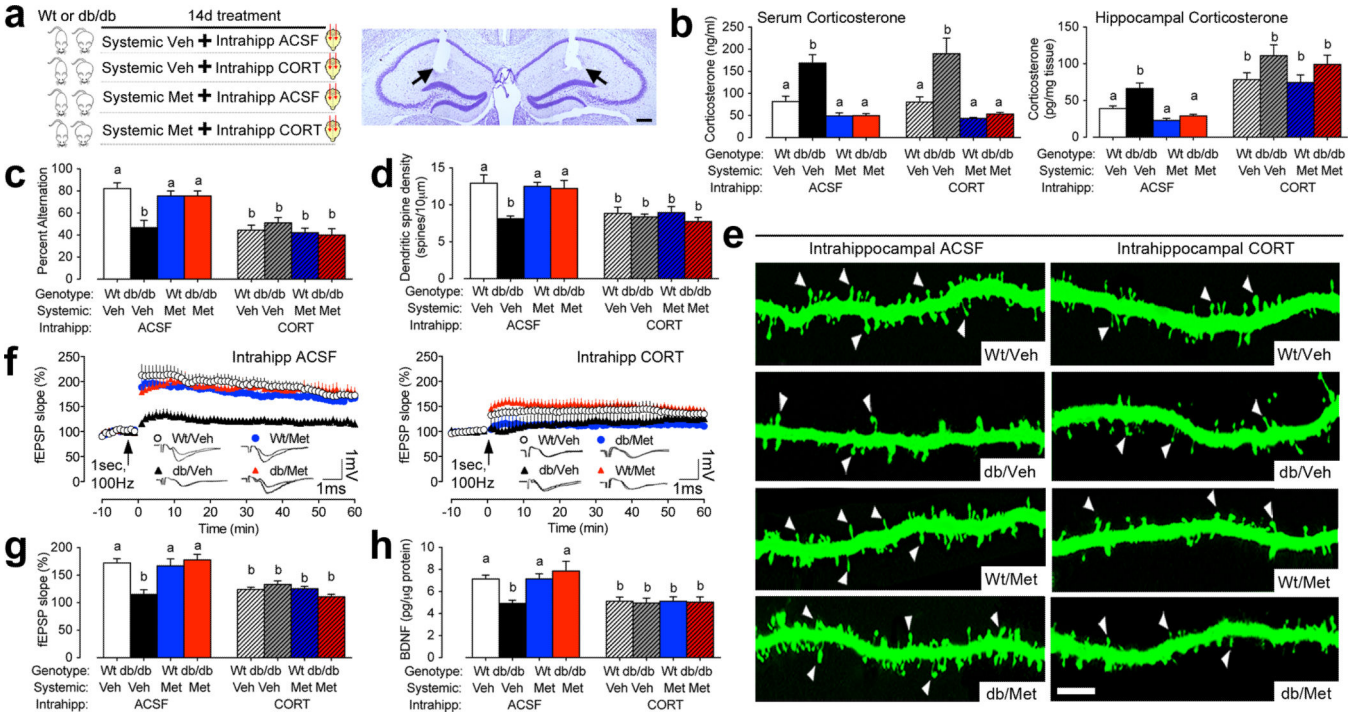

Figure 4. Intrahippocampal exposure to elevated corticosterone levels evokes cognitive and synaptic deficits

(A), Left panel depicts the experimental design. Right panel shows histological section demonstrating bilateral cannula tracks (indicated by arrows) for intrahippocampal corticosterone infusions. Scale bar=100μm. (B, left graph), Systemic metyrapone treatment lowers circulating corticosterone levels in db/db mice in the presence or absence of intrahippocampal corticosterone. (B, right graph), Metyrapone treatment lowers corticosterone levels in the hippocampus of db/db mice, while intrahippocampal corticosterone treatment elevates hippocampal corticosterone levels. Data were analyzed using 2×2×2 ANOVA with post hoc planned comparisons and group differences are indicated by different letters above each bar. (C), Metyrapone treatment rescues spatial alternation in db/db mice infused intrahippocampally with ACSF, while metyrapone and intrahippocampal corticosterone recapitulates cognitive impairment. (D), Quantification of dendritic spine density among dentate gyrus granule cells reveals significant increases in metyrapone-treated db/db mice that were blocked by intrahippocampal corticosterone infusions. (E), Representative micrographs demonstrate that while metyrapone treatment rescues dendritic spine density in db/db mice receiving intrahippocampal ACSF, intrahippocampal corticosterone administration recapitulates spine density deficits. Scale bar=10μm. (F, left graph), Lowering corticosterone levels rescues dentate gyrus long-term potentiation in db/db mice receiving intrahippocampal ACSF. (F, right graph), Intrahippocampal corticosterone treatment impairs LTP in both db/db and wildtype mice, irrespective of systemic glucocorticoid inhibition. (G), Summary graph showing the percent increase in field excitatory postsynaptic potential slope (fEPSP slope) during the last ten minutes of the recording. (H), Intrahippocampal exposure to elevated corticosterone suppresses BDNF protein expression. For all graphs, letters (a, b) indicate statistically significant differences at $p<0.05$ following 2×2×2 ANOVA with Bonferonni's post hoc and

error bars depict the s.e.m. For color interpretation, the reader is referred to the web version of this article.

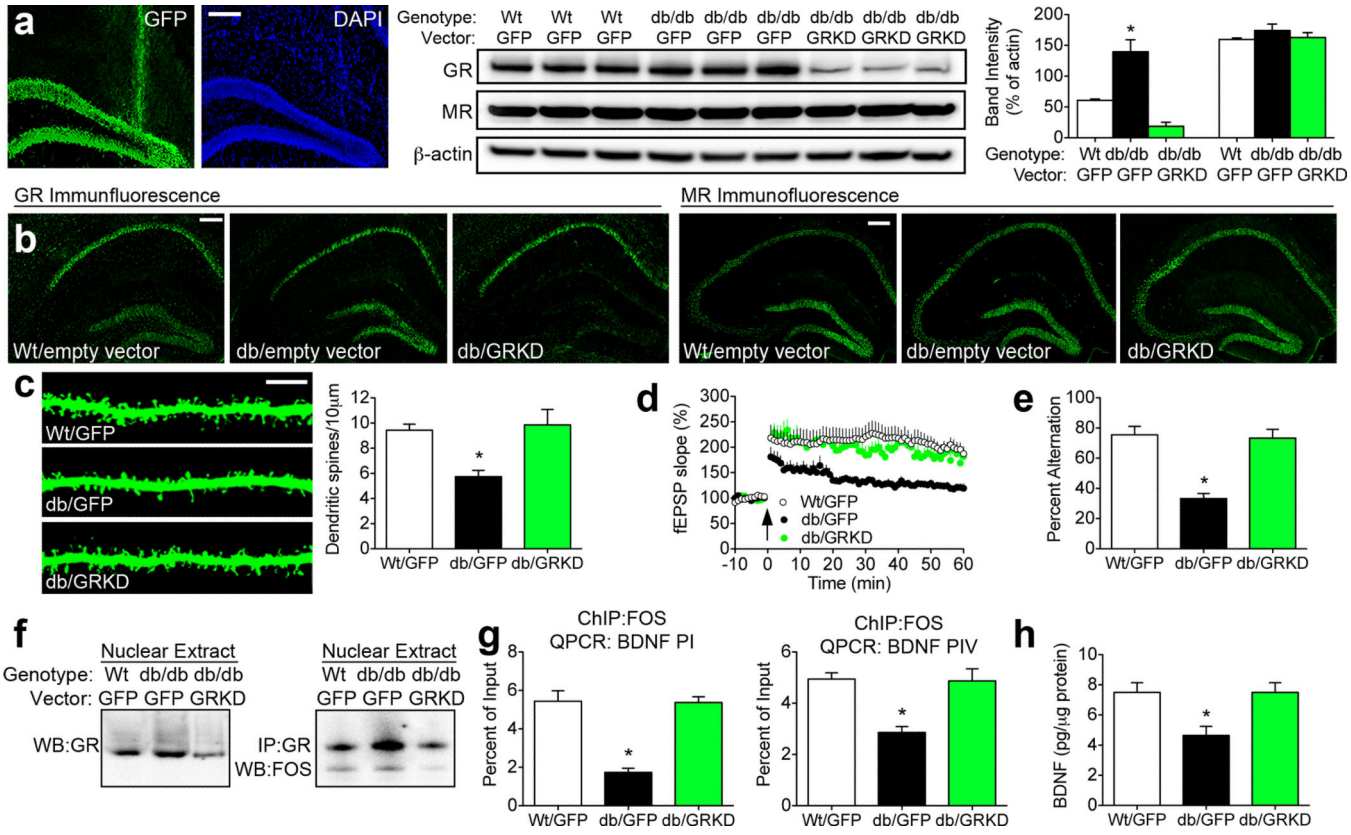

Figure 5. Reducing hippocampal glucocorticoid receptor expression normalizes synaptic plasticity and cognition in db/db mice

(A), Immunofluorescence analysis of the green fluorescent protein (GFP) reporter showing localization to the dentate gyrus subfield. Stereotaxic injection of lentiviral particles bearing GR shRNA reduced hippocampal GR protein expression, with no effect on MR. Graph depicts band intensities normalized to the loading control. (B), Immunofluorescence detection of hippocampal GR revealed selective reductions in immunoreactivity in the dentate gyrus, with no change in MR immunoreactivity. (C), Analysis of dendritic spine density further underscores the involvement of hippocampal GR as a central mediator of structural deficits in db/db mice. Graph shows the mean spine density among dentate gyrus granule cells from animals in each condition. (D), Tetanic stimulation-evoked LTP magnitude is reduced in db/db mice injected with empty vector (encoding GFP), but comparable between db/db mice injected with the GR knockdown vector (GRKD) and wildtype mice. (E), Behavioral analysis of spatial recognition memory in the Y-maze indicates that GR knockdown reinstates hippocampus-dependent learning in db/db mice. (F), Nuclear GR are less abundant in db/db mice injected with the GR knockdown vector, and co-immunoprecipitation revealed reduced binding between GR and Fos, a component of the AP-1 transcription factor complex, after lentiviral suppression of hippocampal GR. (G), Chromatin immunoprecipitation (ChIP) followed by QPCR analysis of BDNF promoters I and IV demonstrated that knocking down GR reinstates the association between Fos protein and BDNF promoter regions. (H), Hippocampal BDNF protein expression is normalized following GR knockdown in db/db mice. For all graphs, asterisk (*) denotes statistical

significance at $p<0.05$ by one-way ANOVA with Bonferonni's post hoc. For color interpretation, the reader is referred to the web version of this article.